

| | |
|--|---|
| | was good ($r=0.85$, $P<0.01$). Conclusion USI seems to be feasible in characterizing BBM in chronic post-stroke spasticity. |
| | |

Author Manuscript

SCHOLARONE™
Manuscripts

This is the author manuscript accepted for publication and has undergone full peer review but has not been through the copyediting, typesetting, pagination and proofreading process, which may lead to differences between this version and the [Version of record](#). Please cite this article as [doi:10.1002/jum.14558](https://doi.org/10.1002/jum.14558).

Ultrasound Strain Imaging to Assess the Biceps Brachii Muscle in Chronic Post-Stroke Spasticity

Jing Gao, MD*^{1,2}, Johnson Chen, MD¹, Michael O'Dell, MD³, Pai-Chi Li, PhD⁴, Wen He, MD⁵,
Li-Juan Du, MD⁵, Jonathan M. Rubin, MD, PhD⁶, William Weitzel, MD⁷, Robert Min, MD¹

1. Department of Radiology, Weill Cornell Medicine, New York, New York, USA
2. Rocky Vista University, Ivins, Utah, USA
3. Rehabilitation Medicine, Weill Cornell Medicine, New York, New York, USA
4. Electric Engineering College, National Taiwan University, Taipei, Taiwan
5. Beijing Tiantan Hospital, Capital Medical University, Beijing, China
6. Department of Radiology, University of Michigan, Ann Arbor, Michigan, USA
7. Veterans Affairs Ann Arbor Health System, Ann Arbor, Michigan, USA

*Corresponding Authors:

Jing Gao, M.D.

Director, Ultrasound in Education and Research

Assistant professor of Ultrasound

Rocky Vista University

255 East Center Street

Room: C286

Telephone: 435-222-1291

Email: jgao@rvu.edu

Acknowledgement: We thank Siemens Medical Solutions for loaning ultrasound scanner to support the study.

Short Title: Ultrasound Strain Imaging to Assess Spastic Muscle

Abstract

Purpose The aim of the study is to assess the feasibility of ultrasound strain imaging (USI) in characterizing biceps brachii muscle (BBM) in chronic post-stroke spasticity.

Methods We prospectively analyzed USI data of bilateral BBM in 8 healthy volunteers and 7 subjects with post-stroke chronic spasticity. The axial deformations of BBM and overlying subcutaneous tissue were produced by external compression using a sandbag (1.0 kg) attached transducer. The lengthening and shortening of BBM and subcutaneous tissue were produced by manual passive elbow extension (from 90° to 0°) and flexion (from 0° to 90°), respectively. We used offline 2-D speckle tracking to estimate axial and longitudinal strain ratios (BBM strain/subcutaneous tissue strain), and longitudinal tissue velocity of BBM. Statistical analyses included ANOVA for testing differences in USI parameters among healthy, non-spastic, and spastic BBMs; Bonferroni correction for further testing differences in USI in the paired groups (healthy vs non-spastic; non-spastic vs spastic; healthy vs non-spastic); and Pearson correlation coefficient for assessing intra-observer reliability of performing USI in stroke survivors.

Results The differences in USI parameters between healthy and spastic, and between non-spastic and spastic BBM were significant at both 90° elbow flexion and maximal elbow extension ($p < 0.01$). There was no significant difference in axial strain ratio at 90° of elbow flexion or longitudinal tissue velocity between healthy and non-spastic BBM ($p > 0.05$). The intra-observer reliability of performing USI in stroke survivors was good ($r=0.85$, $P<0.01$).

Conclusion USI seems to be feasible in characterizing BBM in chronic post-stroke spasticity.

Keywords: Biceps brachii muscle; elastography; post-stroke spasticity; ultrasound strain

Abbreviations: BBM, biceps brachii muscle; ROI, range of interest; ROM, range of motion; USI, ultrasound strain imaging.

Introduction

Approximately two-thirds of 15 million stroke survivors require rehabilitation for the consequences of post-stroke spasticity each year worldwide.¹ Spasticity primarily affects the muscles surrounding the elbow (79%), wrist (66%) and ankle (66%).^{2,3} Accurately characterizing and quantifying the mechanical behavior of spastic muscle may help us better understand the relationship between clinical manifestation and underlying pathophysiology leading to spastic muscle. Furthermore, a reliable measure of spasticity is needed to determine the necessity for and efficacy of potential interventions in clinical management.^{4,5} To date, this remains challenging due to the lack of a gold standard.^{6,7} The commonly used Modified Ashworth Scale (MAS) and Tardieu (TS) in clinical assessment of muscle spasticity are subjective and non-quantitative.⁸ Electromyography (EMG) measures electrical activity of muscles without imaging guidance.⁹ In individuals with post-stroke spasticity, the stiffness increases and motion dynamics decrease in spastic muscle. Post-stroke muscle spasticity and its negative secondary effect (e.g., contractures, limited joint range of motion, and pain) limit musculoskeletal function, which affects their daily living activities.¹⁰⁻¹² It would be ideal to have a noninvasive imaging technique to quantify the mechanical properties and dynamic movement of spastic muscle to assist clinicians in the diagnosis of spasticity, monitoring of disease progression, and evaluation of treatment response in stroke rehabilitation.⁵

Ultrasound strain imaging (USI) has proven to be a useful technique in the assessment of mechanical properties (stiffness) of skeletal muscle.¹³⁻¹⁵ Using 2-D speckle tracking, the axial strain estimates tissue deformation along the ultrasound beam, which is the change in axial tissue length relative to its original length in the direction of the compression.¹⁶⁻¹⁸ The longitudinal strain is the local muscle deformation and displacement parallel to the longitudinal direction of muscle fascicles, resulting from muscle fiber lengthening or shortening produced by passive limb joint movement.¹⁹ The strain is high in “softer” or more elastic tissue and it is low in “stiffer” or less elastic tissue. In individuals with post-stroke spasticity, the stiffness increases and motion dynamics decrease in spastic muscle. Post-stroke muscle spasticity and its negative secondary effect (e.g., contractures, limited joint range of motion, and pain) limit musculoskeletal function, which affects their daily living activities.¹⁰⁻¹² However, little is known about USI technique in assessing skeletal muscle dynamic motion.¹⁹ We have reported the feasibility of USI in determining rigid BBM stiffness in Parkinson’s disease.²⁰ We have also observed high inter-observer and intra-observer agreement of USI in assessing passive BBM dynamic motion in healthy adults.²¹ The aim of this study was to assess the feasibility of USI in assessing spasticity in BBM of stroke survivors.

Materials and Methods

The Internal Review Board at Weill Cornell Medicine approved study (IRB#1601016917) and all subjects provided a written informed consent.

USI of bilateral BBM was performed in 8 healthy volunteers and 8 individuals with post-stroke spasticity of the upper limbs. The study inclusion criteria for healthy controls included:

age 40-60y (an age group with high relevance in regards to vascular events) with normal physical examination; no history of trauma or surgery of the arm; no neuromuscular disorders; and no medication that may affect muscle stiffness and movement. The study inclusion criteria for subjects with chronic post-stroke spasticity included: age > 18y; the time from vascular event to the ultrasound examination was > 6 months;^{4, 7} no history of arm trauma or surgery; ability to sign written informed consent and tolerate passive elbow movement in ultrasound examination, MAS, and TS. All subjects received care from a physician in the Department of Rehabilitation Medicine of Weill Cornell Medicine as standard of care for the treatment of their post-stroke spasticity.

An Acouson S3000 *HELX* equipped with 9L4 linear array transducer (Siemens Medical Solutions, Mountain View, California, USA) was used to acquire grayscale images and real time ultrasound data of BBM deformation and movements.

The subject was placed in the supine position and the arm was relaxed with the forearm supinated. To capture real time ultrasound data of the BBM axial deformation and longitudinal displacement, transmission gel was applied and the ultrasound probe was in long axis placed on the skin elongate with an underlying longitudinal section of the BBM (biceps belly, middle part to distal part of BBM) fiber.²¹ We began scanning with grayscale imaging to observe morphology along a longitudinal section of the BBM. We then acquired real time ultrasound data including bilateral BBM axial deformation and longitudinal displacement sequences.

Real time ultrasound data acquisition

Machine settings for acquiring real time ultrasound data were standardized to capture grayscale imaging cine loops (5-second) of axial deformation and longitudinal displacement of

the BBM. Pre-machine settings for acquiring ultrasound data were standardized, including a maximum image depth of 4 cm, scanning frequency of 7 MHz, single image focus, tissue harmonic imaging, time/space 0, and speckle reduction function turned off to reach real time frame rates as high as > 40 frames per second and to enhance contrast resolution of grayscale image.²¹

BBM axial deformation parallel to the emission sound beam was produced by external compression on the skin and underlying longitudinal section of BBM (Fig. 1a) using a 1.0 kg sandbag tied onto the transducer as the compression force.²¹ The operator held the transducer steady on the underlying skin to avoid out-of-plane motion and any additional force by the operator. A cine loop capturing real time ultrasound data of BBM deformation and relaxation at an elbow angle of 90° (using a 90° angled rest) and at the maximal elbow extension (full extension at 0° elbow angle in healthy controls and possible maximum in stroke survivor) was recorded twice in each BBM.

BBM displacement perpendicular to the emission sound beam was imaged with a free hand (without sandbag) holding the transducer normal to the skin and underlying BBM while an observer manually positioned the elbow in flexion or in extension. Longitudinal strain measurements, displacements, and velocities were measured parallel to the muscle fascicles, which are seen as echogenic bands, in the ultrasound images in the longitudinal orientation (Fig. 1b). A cine loop capturing 5-second real time ultrasound data of passive BBM movement in flexion (elbow angle from 0° to 90°) and in extension (elbow extension from 90° to 0° , or extending maximally without causing the pain) were recorded twice in each BBM. While capturing real time ultrasound data, special attention was paid to avoid any out of plane motion

by both investigator and subject and to maintain elbow motion consistent in order to minimize variation in performing manual elbow flexion and extension.

All real time grayscale image cine loops in Digital Imaging and Communications in Medicine (DICOM) format were exported via universal serial bus (USB) and then transferred to a PC for offline processing.

2-D Speckle tracking to estimate BBM strain and tissue velocity

USI parameters (axial strain, longitudinal strain, and tissue velocity) of BBM (Fig. 1a-b) were estimated using 2-D speckle tracking software (EchoInsight, Epsilon Imaging, Ann Arbor, Michigan, USA). Using phase-sensitive cross-correlation methods for speckle tracking,^{18, 22} the data quality index (DQI, 0-1) is the measure of the frame-to-frame correlation as an indication of the accuracy of motion tracking between frames in axial and lateral directions.²³ In this study, $DQI > 0.9$ (Fig. 1c) is considered valid real time ultrasound data for strain estimation.^{17, 24} We measured BBM strain using the formula of $[(L_1-L_0)/L_0]$, where L_0 is the initial distance and L_1 is the altered distance of the BBM while measured.¹⁶⁻¹⁸

The axial BBM and reference strain represent the anteroposterior deformation in 20 mm BBM and in 5 mm subcutaneous tissue, respectively. Longitudinal BBM and reference strain directly represents one-dimensional tissue lengthening or shortening in 10 mm BBM and in 10 mm subcutaneous tissue, respectively. The relationship between the strain value (the y-axis) and its corresponding time (the x-axis) is displayed as a time-strain curve on a strain graph (Fig. 2 and Fig. 3). A positive strain value (above zero) represents muscle lengthening (elbow extension from 90° to 0°, Fig. 3a and Fig. 3b). A negative strain value (below zero) represents muscle shortening (elbow flexion from 0° to 90°, Fig. 3c and Fig. 3d). In this study, strain ratio (axial

and longitudinal) is the relationship of the maximum strain in BBM (axial or longitudinal) to the maximum strain in the subcutaneous tissue.

In addition, using the correlation coefficient method to track the speckle pattern between matching kernels in the consecutive real time B-mode frames, one-dimensional propagation of mechanical waves and transient tissue velocities during muscle movement can be quantified.^{25,}

²⁶ Longitudinal BBM tissue velocity represents a rapid mechanical lengthening or shortening in longitudinal BBM concentric or eccentric movement. Peak velocity may be considered the most reliable measure for estimating muscle dynamics because the tissue velocity is a *temporal* derivative of tissue displacement. A time-velocity curve (Fig. 4a-4b) displays the magnitude of the longitudinal muscle displacement over time based on the initiation.^{26,27}

A single investigator (JG) successfully performed USI twice for each BBM in all subjects. The time interval between the two ultrasound data acquisitions was 2 minutes. She was blinded to results of MAS and TS examinations.

Modified Ashworth Scale (MAS) and Tardieu Scale (TS)

The MAS and TS were performed on all stroke survivors immediately after ultrasound examinations by an occupational therapist having 10 years' experience in conducting both scales and therapy for post-stroke spasticity. The occupational therapist was blinded to USI result. The

MAS of the arm in one quick stretch is scored as:²⁸

0: no increase in muscle tone.

1: slight increase in muscle tone, manifested by a catch and release or by minimal resistance at the end of the range of motion when the affected part is moved in flexion or extension.

1⁺: slight increase in muscle tone, manifested by a catch, followed by minimal resistance throughout the remainder (less than half) of the region of move.

2: more marked increase in muscle tone through most of the region of move, but easily moved.

3: considerable increase in muscle tone, passive movement difficult.

4: affected part(s) rigid in flexion or extension.

The TS incorporates passive range of motion and quick stretch that is graded as:²⁹

0: No resistance throughout passive movement;

1: Slight resistance throughout passive movement;

2: Clear catch at precise angle, interrupting passive movement, followed by release;

3: Fatigable clonus (a series of involuntary, rhythmic, muscular contractions and relaxations) (less than 10 Sec when maintaining pressure) occurring at a precise angle, followed by release;

4: Sustained clonus (more than 10 Sec when maintaining pressure) occurring at a precise angle.

Statistical analyses

All variables including BBM axial strain, longitudinal strain, tissue velocity, and age of the healthy controls and stroke survivors are characterized by mean and standard deviation (SD).

One-way analysis of variance (ANOVA) was used to test the difference in USI parameters among healthy, non-spastic, and spastic BBM. The Bonferroni correction was then applied to test the difference in the paired groups (healthy vs non-spastic limb in stroke survivors; non-spastic vs spastic; and healthy vs non-spastic).

Box-and-whisker plots are used to display the difference in USI among the healthy, non-spastic, and spastic BBM. Pearson correlation coefficient was applied to test the intra-observer reliability of USI in assessing BBM in stroke survivors. A $p < 0.05$ is considered a statistically significant. Statistical analyses carried out by using SPSS software (SPSS-24.0, SPSS, Chicago, IL) and Microsoft Excel (Excel 13, Microsoft, Redmond, WA).

Results

From February to July 2017, we recruited 8 healthy volunteers (4 men and 4 women, age range 40-56y and mean age 46y) and 8 stroke survivors (5 men and 3 women, age range 34-72y and mean age 59y). The difference in the age between healthy controls and stroke survivors was significant ($p=0.04$). The causes for stroke included intracranial hemorrhage ($n=4$), ischemic infarction ($n=4$). One stroke survivor who did not have upper limb flexor spasticity was excluded from the data analysis. Finally, USI data acquired in 7 subjects with post-stroke BBM spasticity and 8 healthy controls were analyzed. The time period from the stroke to the ultrasound examination ranged from 0.6y - 24y, with an average of 9y. The passive range of motion (ROM) in stroke survivors varied from 130° to 180° , average of 164° . The MAS was scored 2 ($n=4$) and 1^+ ($n=3$) and the TS scored 2 ($n=7$) in the 7 stroke survivors. The DQI for estimating BBM and subcutaneous tissue in all subjects ranged from 0.90 to 0.99, the average DQI was 0.95 (> 0.9 is considered valid data). USI measurements are listed in Table 1. The intra-observer reliability of performing UEI in BBM was good (PCC, $r=0.85$, $p < 0.01$).

We observed a significant increase in muscle stiffness as represented by a remarkable decrease in muscle axial strain in spastic BBM compared with the axial strain in healthy and non-spastic BBMs (all $p < 0.01$, Table 1, Fig. 5a-b). The other component of changes in spastic muscle is neurophysiologic, as passive muscle compliance characterized by muscle lengthening and shortening during passive elbow movement.²⁹ Along these lines we also found impaired BBM dynamic displacement as represented by significant decreases in BBM longitudinal strains (lengthening, Fig. 6a; shortening, Fig. 6b), and tissue velocity (Fig. 7a-b) in spastic BBM compared with healthy and non-spastic BBMs.

Discussion

We report the feasibility of USI in assessing the difference in BBM stiffness and passive dynamic displacement between healthy controls and individuals with chronic post-stroke spasticity.

Central nervous system disorders with upper motor neuron dysfunction often produce spasticity, hypertonia of the limb that is velocity-dependent and dependent on ROM. The elbow flexors (BBM) are most involved and characterized by an increased resistance to passive stretch.⁵ In post-stroke spasticity management, two components of muscle changes have received special attention in neurology and rehabilitation.³⁰ One component of changes in spastic muscle relates to the biomechanical properties, as passive muscle stiffness characterized by the axial deformation of an individual muscle under external compression.³¹ This muscle stiffness is associated with the gain of the stretch reflex and an increase in reflex stiffness, and may contribute to spasticity.³² We observed a significant increase in muscle stiffness as represented by a remarkable decrease in muscle axial strain in spastic BBM compared with the axial strain in healthy and non-spastic BBMs (all $p < 0.01$, Table 1, Fig. 5a-b). The other component of changes in spastic muscle is neurophysiologic, as passive muscle compliance characterized by muscle lengthening and shortening during passive elbow movement.²⁹ Along these lines we also found impaired BBM dynamic displacement as represented by significant decreases in BBM longitudinal strains (lengthening, Fig. 6a; shortening, Fig. 6b), and tissue velocity (Fig. 7a-b) in spastic BBM compared with healthy and non-spastic BBMs.

The explanation for these findings is straightforward. When BBM is spastic, the muscle is stiffer and muscle axial deformation and longitudinal displacement decrease (Table 1).

Changes in spastic BBM is characterized by increased resistance to passive muscle displacement, diminished muscle velocity during elbow extension, and reduced range of muscle displacement. This may be associated with the reduction of fascicle length and the elevation in whole-muscle stiffness in chronic stroke survivors.³³ Although spasticity is neurologic in origin, significant structural adaptations in the soft tissue occur as both changes in muscle cell and extracellular matrix contribute to the limitation of the displacement in spastic muscle.²⁹ Therefore, the increase in stiffness in chronic spastic muscle is often associated with changes in mechanical muscle fiber properties as intramuscular adipose and connective tissue increase.^{13, 30-33} This understandably leads to the decrease in BBM axial strain in USI (Fig. 5) as we observed in the study. In addition, BBM displacement may help evaluate the stretch reflex activity that is strongly associated with function of the skeletal muscle in post-stroke spasticity. There are two parameters that can be used to examine impaired reflex modulation of the BBM, longitudinal strain and tissue velocity. Longitudinal muscle strain shows slower/decreased muscle stretching and shortened muscle length (reduced muscle fiber displacement) at the maximal stretching on a time-strain curve (Fig. 3). Additionally, reduced muscle stretching and increased resistance manifests itself in USI as decreased amplitude of tissue velocity represented in the time-velocity curve (Fig. 4b). A lower tissue velocity may be associated with a hypertonic elbow flexor (BBM) responding to stretch-reflex at slower speeds.³¹ It is important to note that all three USI parameters (axial strain ratio, longitudinal strain ratio, and tissue velocity) are significantly decreased in spastic BBM, and correlated with clinical assessments using MAS ($> 1^+$, increase in muscle tone and resistance to catch) and TS ($=2$, interrupting passive movement).

Interestingly, the difference in axial strain ratio between healthy and non-spastic BBM at maximal elbow extension was significant ($p < 0.05$). The difference in longitudinal strain ratio

during BBM lengthening and shortening between healthy and non-spastic BBM was also significant (all $p < 0.01$). These increases in axial and longitudinal strains in non-spastic BBM may be associated with compensative mechanisms in stroke survivors with spastic BBM impairment, which may lead to mechanical property (axial strain) and function (longitudinal strain) changes in the contralateral muscle.³⁴ However, the difference in BBM longitudinal tissue velocity during lengthening or shortening between healthy and non-spastic BBM (all enrolled stroke survivors with mild BBM spasticity, MAS < 2) was not significant ($p > 0.05$, Fig. 7). The difference in axial strain ratio between healthy and non-spastic BBM at 90° of elbow flexion was not significant either ($p > 0.05$, Fig. 5a). These may result from the similarity of muscle stiffness in the relaxation, stretching resistance, and ROM (reached full elbow extension) in both healthy and non-spastic BBMs.

There are limitations to this study. First, the number of enrolled subjects with post-stroke spasticity is small however significant differences were detected. Second, the difference in the age between healthy controls and stroke survivors was significant. Since muscle shear modulus and strength seem to be affected at ages ≥ 60 y,³⁵ and the average age in this study was 59y, this could have influenced the result to some degree. Third, USI was used to assess chronic post-stroke spasticity and generalizability of these results to acute spasticity is unknown. Fourth, inter-observer agreement in performing USI in post-stroke spasticity was not formally tested, although good intra-observer reproducibility of USI was observed. Fifth, EMG tracing was not used to monitor muscle activity while acquiring real time muscle movement in the study. In addition, the force used to produce muscle deformation and displacement may vary in some degree, even if we used 1.0 kg sand bag as a standard external compression force to produce axial BBM deformation and we normalized BBM axial strain and longitudinal strain using axial

and longitudinal reference subcutaneous strains in all subjects. Finally, BBM movement is three dimensional though we estimated one-dimensional strains of BBM. Therefore, further study using greater numbers of subjects in larger age groups with acute and chronic post-stroke spasticity, and possibility using three dimensional strain techniques will likely provide additional information.

In conclusion, our results suggest that USI is a useful imaging tool in determining increased stiffness and decreased dynamic displacement in spastic BBM by assessing axial strain, longitudinal strain, and tissue velocity of the muscle. These non-invasive USI markers may have potential in improving the point of care management of chronic post-stroke spasticity.

References

1. Thibaut A, Chatelle C, Ziegler E, Bruno MA, Laureys S, Gosseries O. Spasticity after stroke: Physiology, assessment and treatment. *Brain Inj* 2013;27:1093-1105.
2. Wissel J, Schelosky LD, Scott J, Christie W, Faiss JH, Mueller J. Early development of spasticity following stroke: A prospective, observational trial. *J Neurology* 2010;257:1067-1072.
3. Urban PP, Wolf T, Uebele M, Marx JJ, Vogt T, Stoeter P, Bauermann T, Weibrich C, Vucurevic GD, Schneider A, Wissel J. Occurrence and clinical predictors of spasticity after ischemic stroke. *Stroke* 2010;41:2016-2020.
4. Doan QV, Brashear A, Gillard PJ, et al. Relationship between disability and health-related quality of life and caregiver burden in patients with upper limb poststroke spasticity. *Polymyalgia Rheumatica* 2012;4:4-10.

5. Starky A, Sangani SG, McGuire JR, Logan B, Schmit BD. Reliability of biomechanical spasticity measurements at the elbow of people poststroke. *Arch Phys Med Rehabil* 2005;86:1648-1654.
6. Bilston LE and Tan K. Measurement of passive skeletal muscle mechanical properties in vivo: Recent progress, clinical application, and remaining challenges. *Ann Biom Engin* 2015;43:261-73.
7. Sommerfeld DK, Gripenstedt U, Welmer AK. Spasticity after stroke: an overview of prevalence, test instruments, and treatments. *Am J Phys Med Rehabil* 2012;91:814-20.
8. Pisano F, Miscio G, Conte C, Pianca D, Candeloro E, Colombo R. Quantitative measures of spasticity in post-stroke patients. *Clin Neurophysiol* 2000;111:1015-22.
9. Ettiema GJC and Huijing PA. Skeletal muscle stiffness in static and dynamic contractions. *J Biomechanics* 1994;27:1361-8.
10. Thibaut A, Chatelle C, Ziegler E, Bruno MA, Laureys S, Gosseries O. Spasticity after stroke: Physiology, assessment and treatment. *Brain Inj* 2013;27:1093-10
11. Lee SS, Spear S, Rymer WZ. Quantifying changes in material properties of stroke-impaired muscle. *Clin Biomech* 2015;30:269-75.
12. Wu CH, Ho YC, Hsiao MY, Chen WS, Wang TG. Evaluation of post-stroke spasticity muscle stiffness using shear wave ultrasound elastography. *Ultrasound Med Biol* 2017;43:1105-11.
13. Chen EJ, Jenkins WK, O'Brien WD, Jr. Performance of ultrasound speckle tracking in various tissues. *J Acoust Soc Am* 1995;98:1273-8.

14. Chino K, Akagi R, Dohi M, Takahashi H. Measurement of muscle architecture concurrently with muscle hardness using ultrasound strain elastography. *Acta Radiol* 2014;55:833-9.
15. Niitsu M, Michizaki A, Endo A, Takei H, Yanagisawa O. Muscle hardness measurement by using ultrasound elastography: a feasibility study. *Acta Radiol* 2011;52: 99–105.
16. Lubinski MA, Emelianov SY, O'Donnell M. Speckle tracking methods for ultrasonic elasticity imaging using short-time correlation. *IEEE Trans Ultrason Ferroelectr Freq Control* 1999; 46:82-96.
17. Varghese T. Quasi-static ultrasound elastography. *Ultrasound Clin* 2009; 4:323-38.
18. O'Donnell M, Skovoroda AR, Shapo BM, Emelianov SY. Internal displacement and strain imaging using ultrasound speckle tracking. *IEEE Trans Ultrason Ferroelectr Freq Contr.* 1994; 41:314-25
19. Sikder S, Wei Q, Cortes N. Dynamic ultrasound imaging application to quantify musculoskeletal function. *Exerc Sport Sci Rev* 2014; 42:125-35.
20. Gao J, He W, Du LJ, et al. Ultrasound Strain Elastography in Assessment of Resting Biceps Brachii Muscle Stiffness in Patients with Parkinson's disease: A Primary Observation. *Clin Imaging* 2016; 40:440-4
21. Gao J, Li PC, Chen J, et al. Ultrasound strain imaging in assessment of biceps muscle stiffness and dynamic motion in healthy adults. *Ultrasound Med Biol* 2017; 43:1729-36.
22. Kaluzynski K, Chen XC, Emelianov SY, Skovoroda AR, O'Donnell M. Strain rate imaging using two-dimensional speckle tracking. *IEEE Trans Ultrason Ferroelectr Freq Contr* 2001; 48:1111-23.

23. Patel P, Biswas R, Park DW, et al. Characterization of vascular strain during in-vitro angioplasty with high-resolution ultrasound speckle tracking. *Theoretical Biology and Medical Modelling* 2010; 7:36.
24. D'hooge J, Heimdal A, Jamal F, et al. Regional strain and strain rate measurements by cardiac ultrasound: principle, implementation, and limitations. *Eur J Echocardiogr* 2000; 1:154-70.
25. Grönlund C, Claesson K, Holtermann A. Imaging two-dimensional mechanical wave of skeletal muscle contraction. *Ultrasound Med Biol* 2013;39:360-9.
26. Peolsson M, Brodin LA, Peolsson A. Tissue motion pattern of ventral neck muscles investigated by tissue velocity ultrasonography imaging. *Eur J Appl Physiol* 2010; 109:899-908.
27. Lindberg F, Mårtensson M, Grönlund C, Brodin LA. Evaluation of ultrasound tissue velocity imaging: a phantom study of velocity estimation in skeletal muscle low-level contraction. *BMC Medical Imaging* 2013; 13:16. DOI: 10.1186/1471-2342-13-16.
28. Pandyan AD, Price CI, Barnes MP, Johnson GR. A biomechanical investigation into the validity of the modified Ashworth scale as a measure of elbow spasticity. *Clin Rehabil* 2003;17:290–3.
29. Haugh AB, Pandyan AD, Johnson GR. A systematic review of the Tardieu Scale for the measurement of spasticity. *Disabil Rehabil* 2006;28:899-907.
30. Lieber RL, Ward SR. Cellular mechanisms of tissue fibrosis: 4. Structural and functional consequences of skeletal muscle fibrosis. *Am J Physiol Cell Physiol* 2013;305:C241–252.
31. Mayer N, Esquenazi A, Childers M. Common patterns of clinical motor dysfunction. *Muscle and Nerve* 1997;6:S21-35.

32. Thilmann AF, Fellows SJ, Garms E. The mechanism of spastic muscle hypertonus. Variation in reflex gain over the time course of spasticity. *Brain* 1991;114:233-244.
33. Gao F, Grant TH, Roth EJ, et al: Changes in passive mechanical properties of the gastrocnemius muscle at the muscle fascicle and joint levels in stroke survivors. *Arch Phys Med Rehabil* 2009;90:819-826.
34. Lorentzen J, Grey MJ, Crone C, Mazevet D, Biering-Sørensen F, Nielsen JB. Distinguishing active from passive components of ankle plantar flexor stiffness in stroke, spinal cord injury and multiple sclerosis. *Clin Neurophysiology* 2010;121:1939-51.
35. Eby SF, Cloud BA, Brandenburg JE, et al. Shear wave elastography of passive skeletal muscle stiffness: Influences of sex and age throughout adulthood. *Clin Biomechanics* 2015;30:22-7.

Table 1. USI parameters of biceps brachii muscle in 8 healthy controls and 7 stroke survivors

| Parameters | Healthy | Non-spastic BBM | Spastic BBM | ANOVA (F*/P) |
|-------------------------------------|------------|-----------------|-------------|------------------|
| Maximal elbow extension | 180° | 180° | 164°± | 9.10/ 0.001 |
| Axial strain ratio (90°) | 4.71±0.06 | 4.87±0.04 | 3.13±0.46 | 102.39/ < 0.0001 |
| Axial strain ratio (0°) | 3.32±0.04 | 4.02±0.05 | 2.65±0.04 | 1976/ < 0.0001 |
| Longitudinal strain ratio (90°- 0°) | 4.56±0.06 | 5.79±1.49 | 3.12±0.68 | 15.96/ < 0.0001 |
| Longitudinal strain ratio (0°- 90°) | 4.77±0.06 | 6.56±0.31 | 3.25±0.74 | 101.78/ < 0.0001 |
| Tissue velocity (90°- 0°) | 2.14±0.48 | 2.16±0.6 | 1.33±0.45 | 6.79/ 0.005 |
| Tissue velocity (0°- 90°) | -2.11±0.63 | -2.09±0.29 | -0.95±0.31 | 18.34/ < 0.0001 |

Note: 90° and 0° indicated the angle of elbow at 90° of flexion and 0° of flexion (full extension).

*F value = variance of the group means (Mean Square Between) / mean of the within group variance (Mean Squared Error).

Figure legends

Fig. 1a-c Real time grayscale images of longitudinal section of the biceps brachii muscle (BBM) and subcutaneous tissue were captured for offline strain estimation. Using 2-D speckle tracking, the regions of interest for estimating axial and longitudinal BBM (reference) strains are selected. a. BBM axial strain represents deformations along the direction of emission sound beam in 20 mm anteroposterior region (cyan, red, and yellow dotted lines) of the muscle and reference axial strain represents the deformation in 5 mm anteroposterior subcutaneous soft tissue (purple dotted line) under external compression. b. Longitudinal strain estimates the tissue displacement moving perpendicular to the direction of emission sound beam and elongation with muscle fiber and fascicles (yellow arrow) following manual elbow extension (from 90° to 0°) and flexion (from 0° to 90°). BBM and reference longitudinal strains represent longitudinal displacements in 10 mm of muscle (red dotted line) and 10 mm of subcutaneous tissue (cyan dotted line), respectively. c. Data quality index (DQI) is used to assess the reliability of acquired real time ultrasound data for estimating tissue strain using correlation coefficient method in speckle tracking. $DQI > 0.95$ in this graph indicates that real time ultrasound data are valid for strain estimation.

Fig. 2a-b The time-strain graphs display the relationship of axial biceps brachii muscle (BBM) strain to axial subcutaneous soft tissue (reference) strain estimated using 2-D speckle tracking software. Axial

strain ratio is defined as the average of 3 BBM strains (cyan, red, and yellow dotted lines) divided by the reference strain (purple line). There is an apparent significant difference in axial strain ratio between BBM in a 56-year-old healthy volunteer (a) and in a 42-year-old stroke survivor (b) with MAS =2 and Tardieu Scale =2 (axial strain ratio 5.2 vs 3.1). The difference in reference strain between two subjects is not significant. The result suggests that the spastic BBM is stiffer and less elastic than the healthy BBM. In the strain graphs, the X-axis is the time in seconds and the Y-axis is the value of the strain.

Fig. 3a-d These time-strain graphs show longitudinal strains of the biceps brachii muscle (BBM) and reference subcutaneous tissue during manual elbow movement and estimated using 2-D speckle tracking software (Fig. 1b). A positive strain value (above zero) represents tissue lengthening during extension of the elbow angle from 90° to 0° (a and b). A negative strain value (below zero) represents tissue shortening during flexion of the elbow angle from 0° to 90° (c and d). Longitudinal strain ratio is defined as BBM strain divided by the reference strain. Longitudinal strain ratio is significantly higher in a healthy BBM (a and c) than in a spastic BBM with MAS =1⁺ and Tardieu Scale =2 (b and d) during elbow extension (a vs b) and during elbow flexion (c vs d). In the strain graphs, the X-axis is the time in seconds and the Y-axis is the value of the strain.

Fig. 4a-b Time-velocity graphs show biceps brachii muscle (BBM, red line) tissue velocity and subcutaneous tissue velocity (cyan line) during tissue lengthening (elbow extension from 90° to 0°). The notion is that peak BBM tissue velocity is significantly higher in healthy BBM (a) than in spastic BBM (b) (2.9 cm/se vs 1.7 cm/sec). It should be noted that the velocity scale in graph a (2.5 cm/sec) is different from that in graph b (1.0 cm/sec). In the time-velocity graphs, the x-axis is the time in seconds and the y-axis is value of velocity (cm/sec).

Fig. 5a-b. Box-and-whisker plots illustrate the axial strain ratios of spastic (black colored box), non-spastic (green colored box), and healthy (orange colored box) biceps brachii muscles (BBM) at elbow joint angle of 90° (a) and 0° or maximal achieved extension angle in post-stroke subjects (b). The axial strain ratio in spastic BBM is significantly lower than healthy and non-spastic BBM (Table 1). The difference in axial strain ratio between healthy and non-spastic BBM is also significant at elbow extension (elbow angle of 0°), but it is not at the elbow flexion angle of 90°.

Fig. 6a-b. Box-and-whisker plots illustrate the Longitudinal strain ratios of spastic (black colored box), non-spastic (green colored box), and healthy (orange colored box) biceps brachii muscle (BBM) to reference tissue produced by elbow flexion from 0° to 90° (a) and elbow extension from 90° to 0° (b). The longitudinal strain ratio in spastic BBM is significantly lower than healthy and non-spastic BBM (Table 1). The difference in longitudinal strain ratio between healthy and non-spastic BBM at extension and flexion is also significant ($p < 0.05$).

Fig. 7a-b. Box-and-whisker plots illustrate peak tissue velocity (cm/sec) in spastic (black colored box), non-spastic (green colored box), and healthy (orange colored box) biceps brachii muscle (BBM) during elbow extension from 90° to 0° (a, positive velocity value represents muscle lengthening) and during elbow flexion from 0° to 90° (b, negative velocity value represents muscle shortening). One can clearly note that the peak BBM velocity in spastic BBM is significantly lower than healthy and non-spastic BBM (Table. 1) during extension and flexion. The difference in tissue velocity between healthy and non-spastic BBM is not significant ($p > 0.05$).

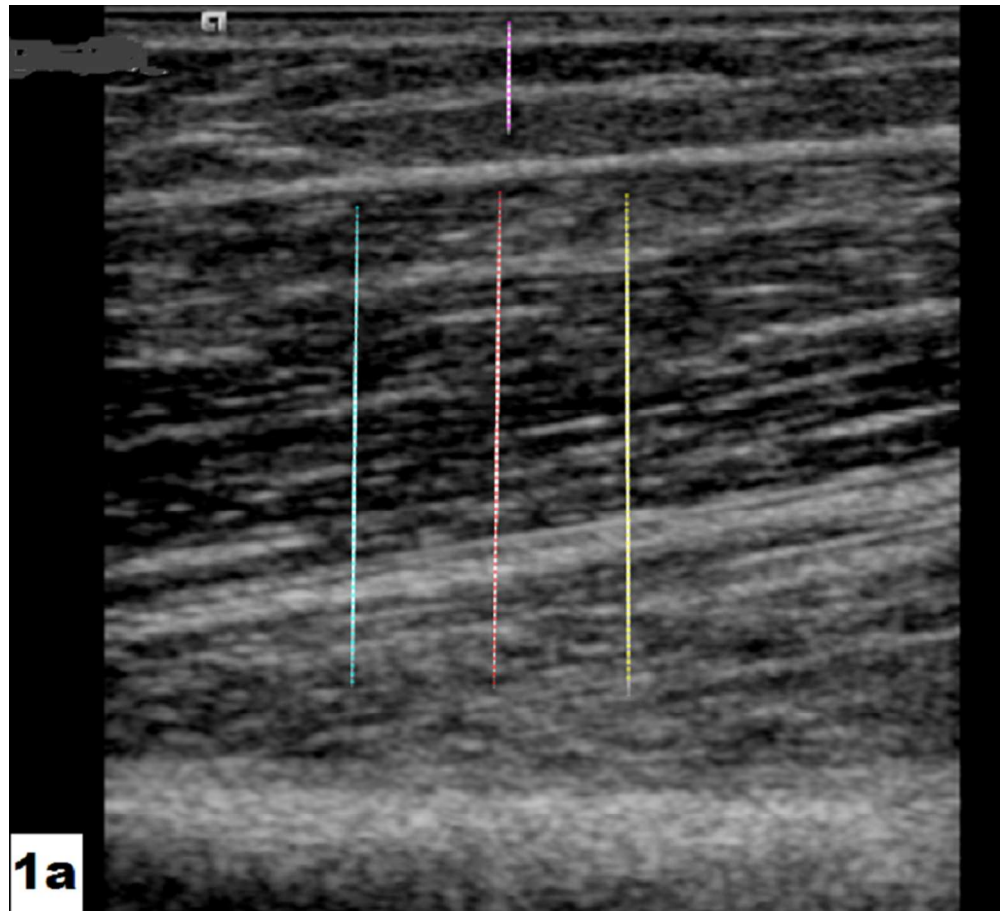


Fig. 1a-c Real time grayscale images of longitudinal section of the biceps brachii muscle (BBM) and subcutaneous tissue were captured for offline strain estimation. Using 2-D speckle tracking, the regions of interest for estimating axial and longitudinal BBM (reference) strains are selected. a. BBM axial strain represents deformations along the direction of emission sound beam in 20 mm anteroposterior region (cyan, red, and yellow dotted lines) of the muscle and reference axial strain represents the deformation in 5 mm anteroposterior subcutaneous soft tissue (purple dotted line) under external compression. b. Longitudinal strain estimates the tissue displacement moving perpendicular to the direction of emission sound beam and elongation with muscle fiber and fascicles (yellow arrow) following manual elbow extension (from 90° to 0°) and flexion (from 0° to 90°). BBM and reference longitudinal strains represent longitudinal displacements in 10 mm of muscle (red dotted line) and 10 mm of subcutaneous tissue (cyan dotted line), respectively. c. Data quality index (DQI) is used to assess the reliability of acquired real time ultrasound data for estimating tissue strain using correlation coefficient method in speckle tracking. $DQI > 0.95$ in this graph indicates that real time ultrasound data are valid for strain estimation.

77x70mm (300 x 300 DPI)

AJ

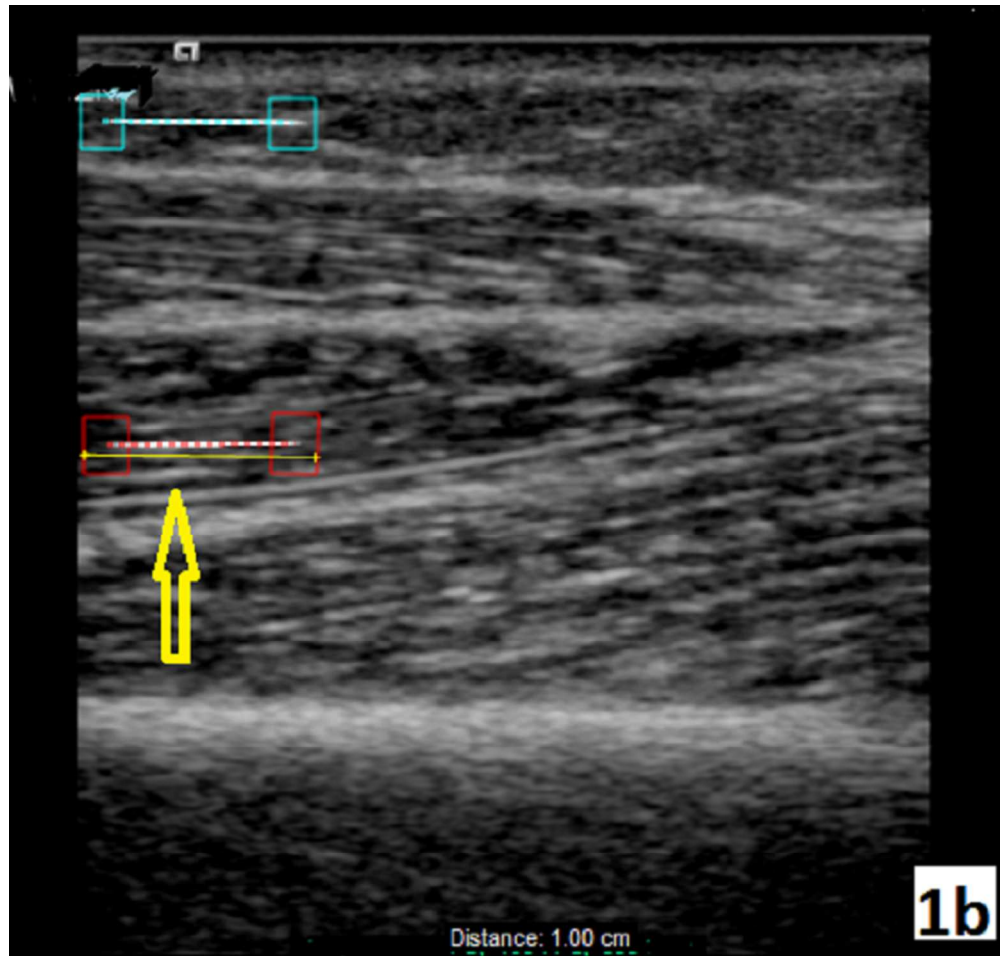


Fig. 1a-c Real time grayscale images of longitudinal section of the biceps brachii muscle (BBM) and subcutaneous tissue were captured for offline strain estimation. Using 2-D speckle tracking, the regions of interest for estimating axial and longitudinal BBM (reference) strains are selected. a. BBM axial strain represents deformations along the direction of emission sound beam in 20 mm anteroposterior region (cyan, red, and yellow dotted lines) of the muscle and reference axial strain represents the deformation in 5 mm anteroposterior subcutaneous soft tissue (purple dotted line) under external compression. b. Longitudinal strain estimates the tissue displacement moving perpendicular to the direction of emission sound beam and elongation with muscle fiber and fascicles (yellow arrow) following manual elbow extension (from 90° to 0°) and flexion (from 0° to 90°). BBM and reference longitudinal strains represent longitudinal displacements in 10 mm of muscle (red dotted line) and 10 mm of subcutaneous tissue (cyan dotted line), respectively. c. Data quality index (DQI) is used to assess the reliability of acquired real time ultrasound data for estimating tissue strain using correlation coefficient method in speckle tracking. $DQI > 0.95$ in this graph indicates that real time ultrasound data are valid for strain estimation.

77x74mm (300 x 300 DPI)

A

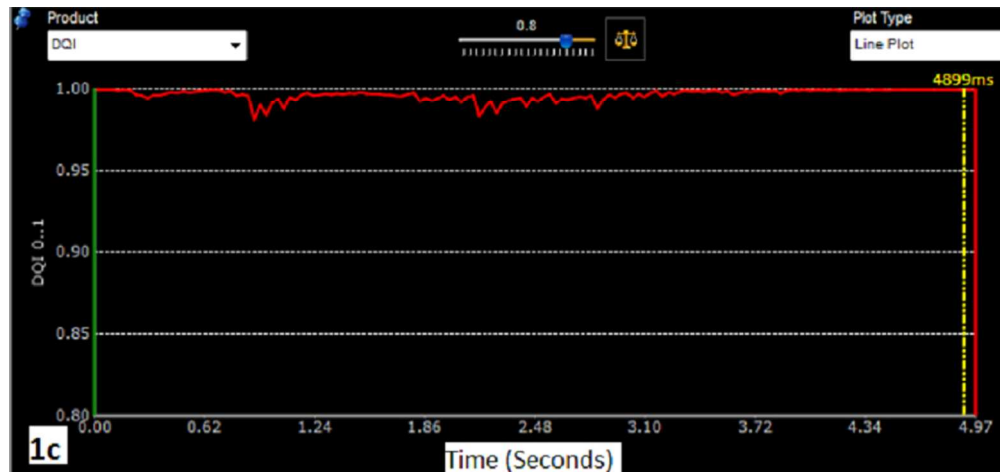


Fig. 1a-c Real time grayscale images of longitudinal section of the biceps brachii muscle (BBM) and subcutaneous tissue were captured for offline strain estimation. Using 2-D speckle tracking, the regions of interest for estimating axial and longitudinal BBM (reference) strains are selected. a. BBM axial strain represents deformations along the direction of emission sound beam in 20 mm anteroposterior region (cyan, red, and yellow dotted lines) of the muscle and reference axial strain represents the deformation in 5 mm anteroposterior subcutaneous soft tissue (purple dotted line) under external compression. b. Longitudinal strain estimates the tissue displacement moving perpendicular to the direction of emission sound beam and elongation with muscle fiber and fascicles (yellow arrow) following manual elbow extension (from 90° to 0°) and flexion (from 0° to 90°). BBM and reference longitudinal strains represent longitudinal displacements in 10 mm of muscle (red dotted line) and 10 mm of subcutaneous tissue (cyan dotted line), respectively. c. Data quality index (DQI) is used to assess the reliability of acquired real time ultrasound data for estimating tissue strain using correlation coefficient method in speckle tracking. DQI > 0.95 in this graph indicates that real time ultrasound data are valid for strain estimation.

77x36mm (300 x 300 DPI)

Author

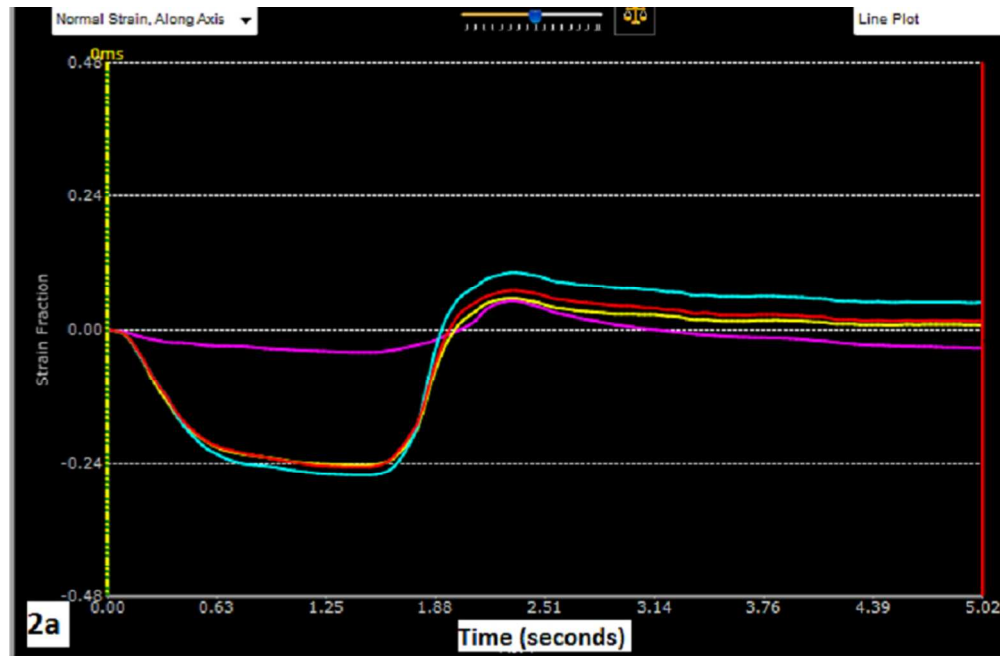


Fig. 2a-b The time-strain graphs display the relationship of axial biceps brachii muscle (BBM) strain to axial subcutaneous soft tissue (reference) strain estimated using 2-D speckle tracking software. Axial strain ratio is defined as the average of 3 BBM strains (cyan, red, and yellow dotted lines) divided by the reference strain (purple line). There is an apparent significant difference in axial strain ratio between BBM in a 56-year-old healthy volunteer (a) and in a 42-year-old stroke survivor (b) with MAS =2 and Tardieu Scale =2 (axial strain ratio 5.2 vs 3.1). The difference in reference strain between two subjects is not significant. The result suggests that the spastic BBM is stiffer and less elastic than the healthy BBM. In the strain graphs, the X-axis is the time in seconds and the Y-axis is the value of the strain.

77x50mm (300 x 300 DPI)

Autho1

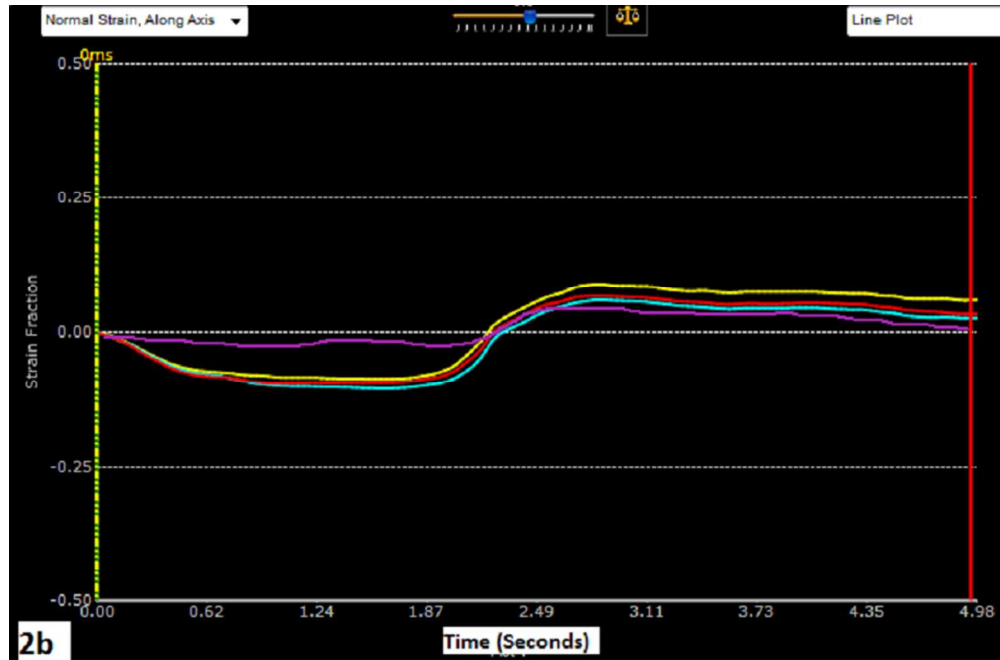


Fig. 2a-b The time-strain graphs display the relationship of axial biceps brachii muscle (BBM) strain to axial subcutaneous soft tissue (reference) strain estimated using 2-D speckle tracking software. Axial strain ratio is defined as the average of 3 BBM strains (cyan, red, and yellow dotted lines) divided by the reference strain (purple line). There is an apparent significant difference in axial strain ratio between BBM in a 56-year-old healthy volunteer (a) and in a 42-year-old stroke survivor (b) with MAS =2 and Tardieu Scale =2 (axial strain ratio 5.2 vs 3.1). The difference in reference strain between two subjects is not significant. The result suggests that the spastic BBM is stiffer and less elastic than the healthy BBM. In the strain graphs, the X-axis is the time in seconds and the Y-axis is the value of the strain.

77x51mm (300 x 300 DPI)

Authoi

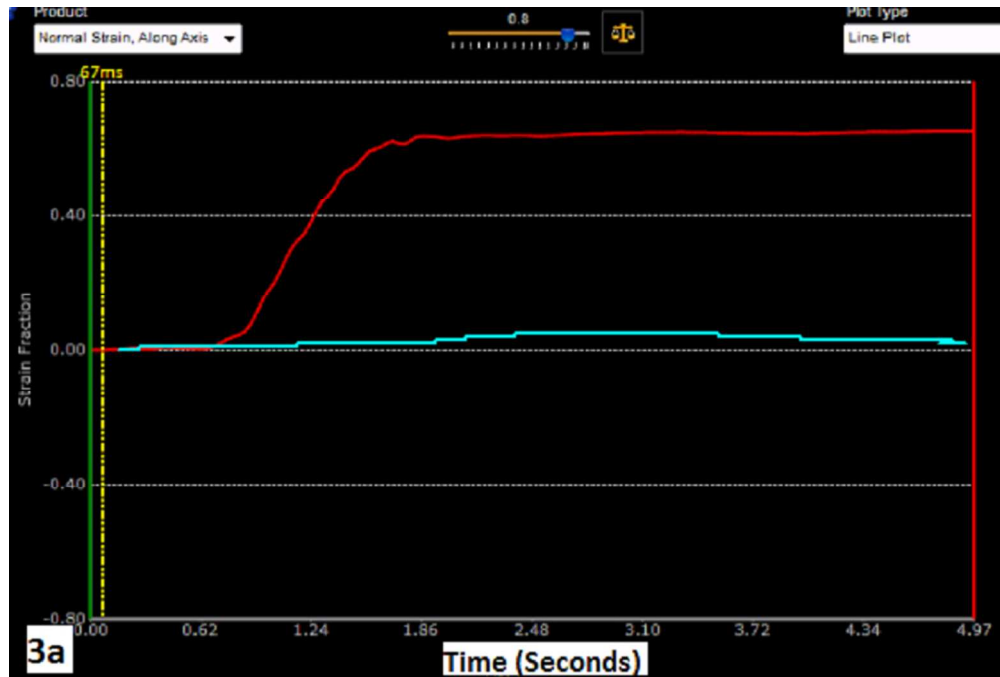


Fig. 3a-d These time-strain graphs show longitudinal strains of the biceps brachii muscle (BBM) and reference subcutaneous tissue during manual elbow movement and estimated using 2-D speckle tracking software (Fig. 1b). A positive strain value (above zero) represents tissue lengthening during extension of the elbow angle from 90° to 0° (a and b). A negative strain value (below zero) represents tissue shortening during flexion of the elbow angle from 0° to 90° (c and d). Longitudinal strain ratio is defined as BBM strain divided by the reference strain. Longitudinal strain ratio is significantly higher in a healthy BBM (a and c) than in a spastic BBM with MAS =1+ and Tardieu Scale =2 (b and d) during elbow extension (a vs b) and during elbow flexion (c vs d). In the strain graphs, the X-axis is the time in seconds and the Y-axis is the value of the strain.

77x52mm (300 x 300 DPI)

Autho

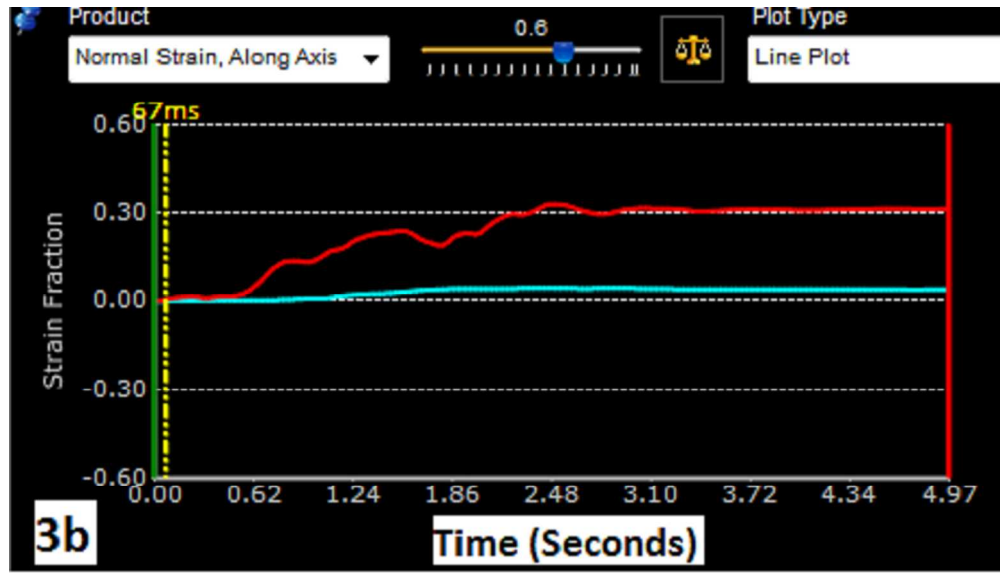


Fig. 3a-d These time-strain graphs show longitudinal strains of the biceps brachii muscle (BBM) and reference subcutaneous tissue during manual elbow movement and estimated using 2-D speckle tracking software (Fig. 1b). A positive strain value (above zero) represents tissue lengthening during extension of the elbow angle from 90° to 0° (a and b). A negative strain value (below zero) represents tissue shortening during flexion of the elbow angle from 0° to 90° (c and d). Longitudinal strain ratio is defined as BBM strain divided by the reference strain. Longitudinal strain ratio is significantly higher in a healthy BBM (a and c) than in a spastic BBM with MAS =1+ and Tardieu Scale =2 (b and d) during elbow extension (a vs b) and during elbow flexion (c vs d). In the strain graphs, the X-axis is the time in seconds and the Y-axis is the value of the strain.

77x44mm (300 x 300 DPI)

Author

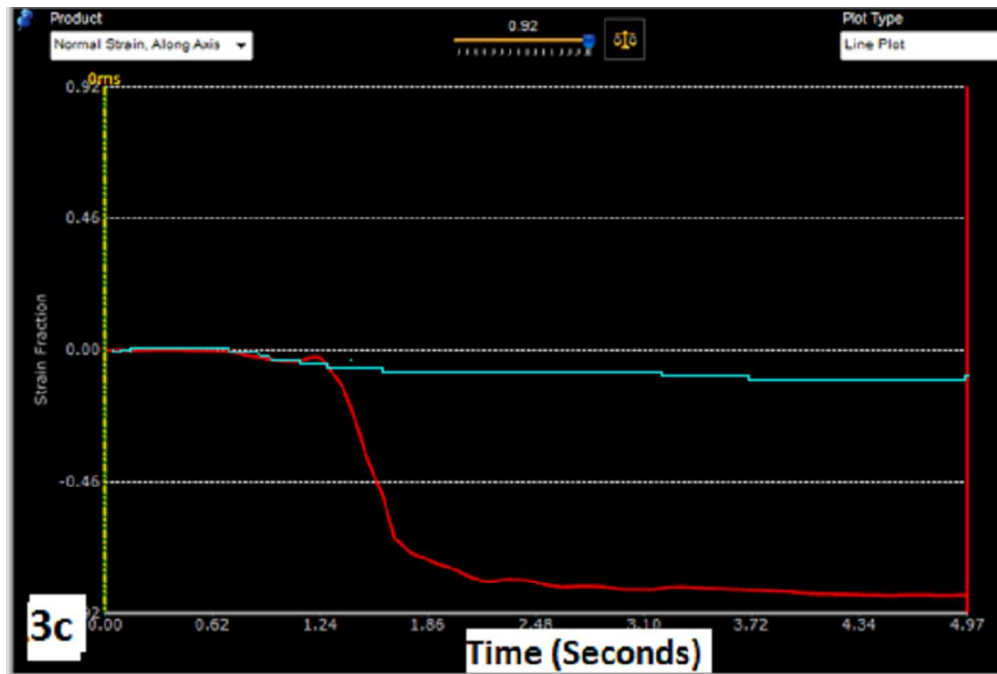


Fig. 3a-d These time-strain graphs show longitudinal strains of the biceps brachii muscle (BBM) and reference subcutaneous tissue during manual elbow movement and estimated using 2-D speckle tracking software (Fig. 1b). A positive strain value (above zero) represents tissue lengthening during extension of the elbow angle from 90° to 0° (a and b). A negative strain value (below zero) represents tissue shortening during flexion of the elbow angle from 0° to 90° (c and d). Longitudinal strain ratio is defined as BBM strain divided by the reference strain. Longitudinal strain ratio is significantly higher in a healthy BBM (a and c) than in a spastic BBM with MAS =1+ and Tardieu Scale =2 (b and d) during elbow extension (a vs b) and during elbow flexion (c vs d). In the strain graphs, the X-axis is the time in seconds and the Y-axis is the value of the strain.

77x52mm (300 x 300 DPI)

Autho

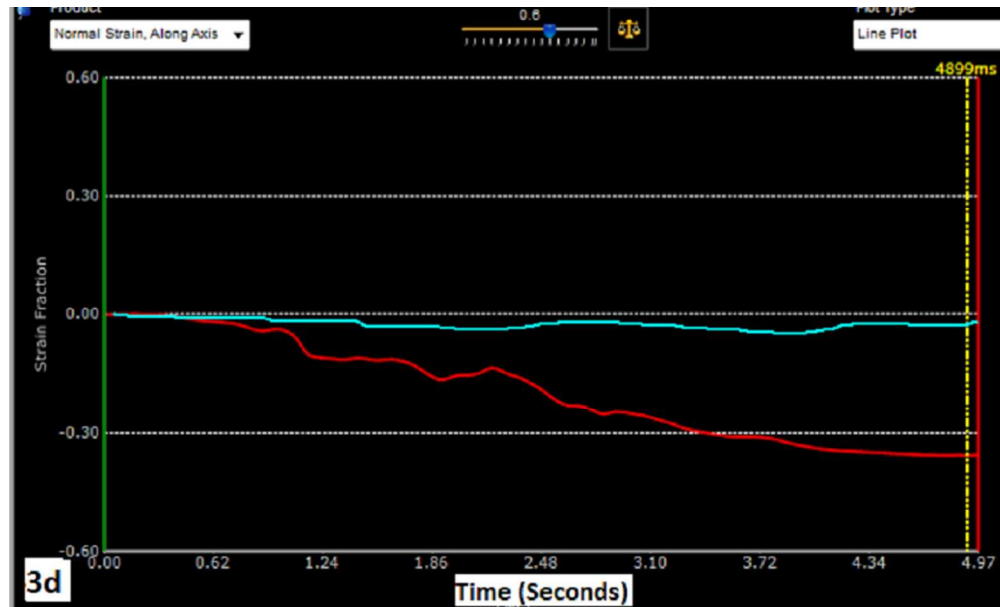


Fig. 3a-d These time-strain graphs show longitudinal strains of the biceps brachii muscle (BBM) and reference subcutaneous tissue during manual elbow movement and estimated using 2-D speckle tracking software (Fig. 1b). A positive strain value (above zero) represents tissue lengthening during extension of the elbow angle from 90° to 0° (a and b). A negative strain value (below zero) represents tissue shortening during flexion of the elbow angle from 0° to 90° (c and d). Longitudinal strain ratio is defined as BBM strain divided by the reference strain. Longitudinal strain ratio is significantly higher in a healthy BBM (a and c) than in a spastic BBM with MAS =1+ and Tardieu Scale =2 (b and d) during elbow extension (a vs b) and during elbow flexion (c vs d). In the strain graphs, the X-axis is the time in seconds and the Y-axis is the value of the strain.

77x46mm (300 x 300 DPI)

Author

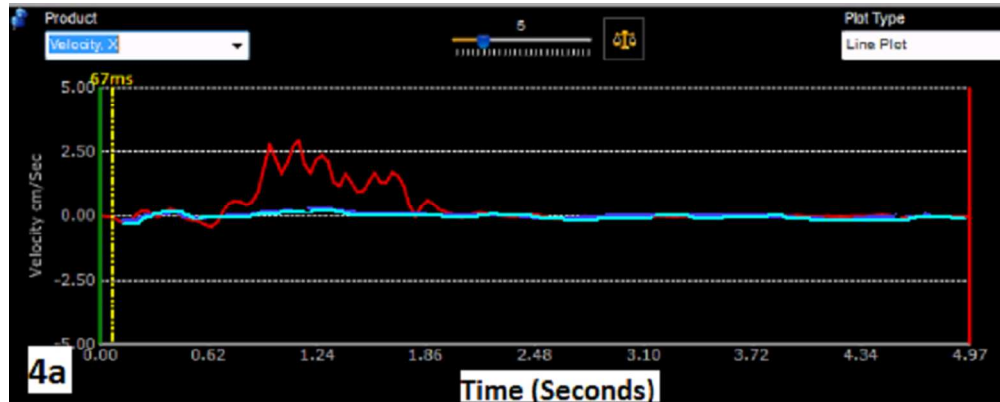


Fig. 4a-b Time-velocity graphs show biceps brachii muscle (BBM, red line) tissue velocity and subcutaneous tissue velocity (cyan line) during tissue lengthening (elbow extension from 90° to 0°). The notion is that peak BBM tissue velocity is significantly higher in healthy BBM (a) than in spastic BBM (b) (2.9 cm/se vs 1.7 cm/sec). It should be noted that the velocity scale in graph a (2.5 cm/sec) is different from that in graph b (1.0 cm/sec). In the time-velocity graphs, the x-axis is the time in seconds and the y-axis is value of velocity (cm/sec).

77x31mm (300 x 300 DPI)

Author Mā

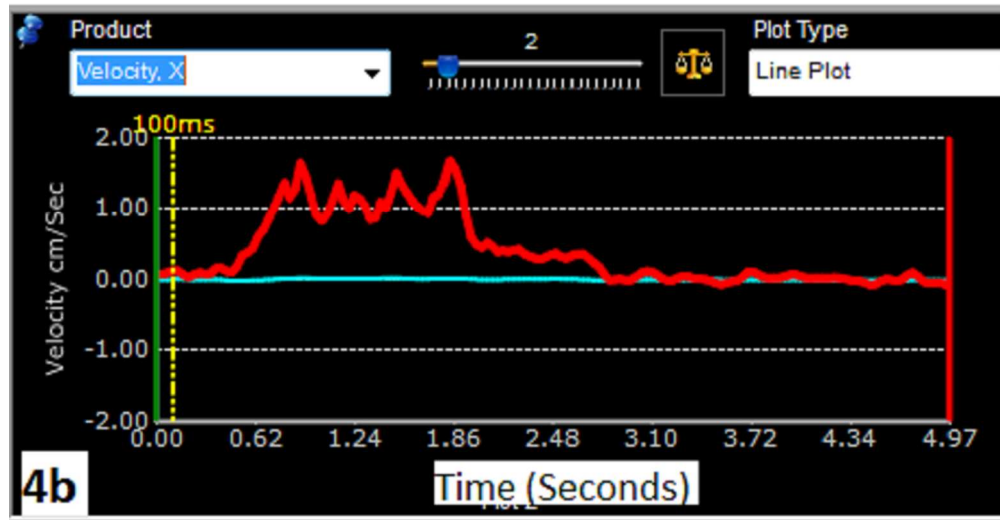


Fig. 4a-b Time-velocity graphs show biceps brachii muscle (BBM, red line) tissue velocity and subcutaneous tissue velocity (cyan line) during tissue lengthening (elbow extension from 90° to 0°). The notion is that peak BBM tissue velocity is significantly higher in healthy BBM (a) than in spastic BBM (b) (2.9 cm/se vs 1.7 cm/sec). It should be noted that the velocity scale in graph a (2.5 cm/sec) is different from that in graph b (1.0 cm/sec). In the time-velocity graphs, the x-axis is the time in seconds and the y-axis is value of velocity (cm/sec).

77x40mm (300 x 300 DPI)

Author N

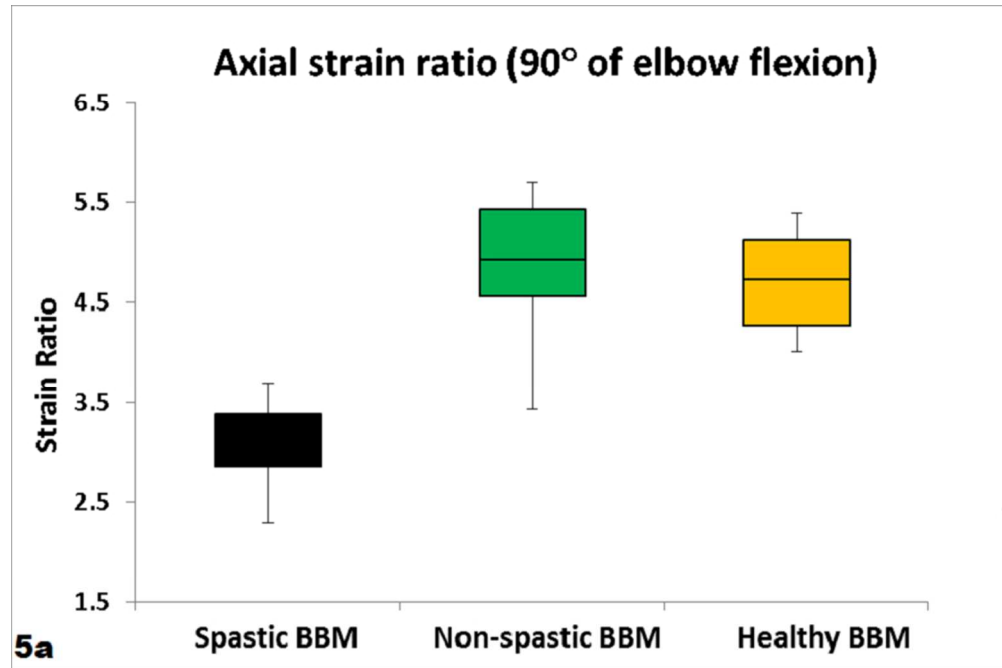


Fig. 5a-b. Box-and-whisker plots illustrate the axial strain ratios of spastic (black colored box), non-spastic (green colored box), and healthy (orange colored box) biceps brachii muscles (BBM) at elbow joint angle of 90° (a) and 0° or maximal achieved extension angle in post-stroke subjects (b). The axial strain ratio in spastic BBM is significantly lower than healthy and non-spastic BBM (Table 1). The difference in axial strain ratio between healthy and non-spastic BBM is also significant at elbow extension (elbow angle of 0°), but it is not at the elbow flexion angle of 90°.

77x51mm (300 x 300 DPI)

Author

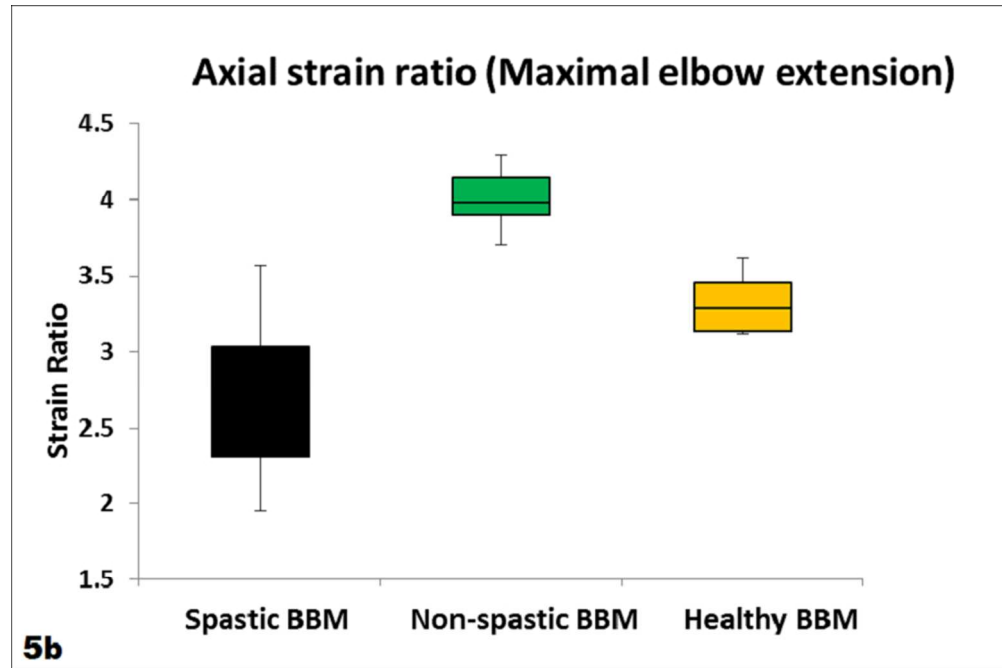


Fig. 5a-b. Box-and-whisker plots illustrate the axial strain ratios of spastic (black colored box), non-spastic (green colored box), and healthy (orange colored box) biceps brachii muscles (BBM) at elbow joint angle of 90° (a) and 0° or maximal achieved extension angle in post-stroke subjects (b). The axial strain ratio in spastic BBM is significantly lower than healthy and non-spastic BBM (Table 1). The difference in axial strain ratio between healthy and non-spastic BBM is also significant at elbow extension (elbow angle of 0°), but it is not at the elbow flexion angle of 90° .

77x51mm (300 x 300 DPI)

Author

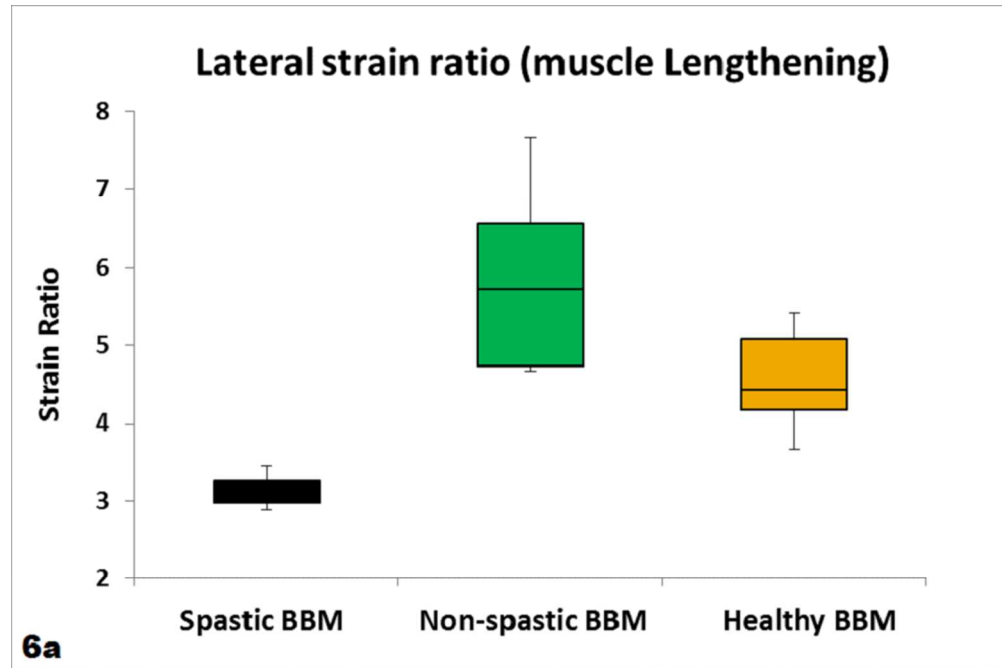


Fig. 6a-b. Box-and-whisker plots illustrate the Longitudinal strain ratios of spastic (black colored box), non-spastic (green colored box), and healthy (orange colored box) biceps brachii muscle (BBM) to reference tissue produced by elbow flexion from 0° to 90° (a) and elbow extension from 90° to 0° (b). The longitudinal strain ratio in spastic BBM is significantly lower than healthy and non-spastic BBM (Table 1). The difference in longitudinal strain ratio between healthy and non-spastic BBM at extension and flexion is also significant ($p < 0.05$).

77x51mm (300 x 300 DPI)

Author

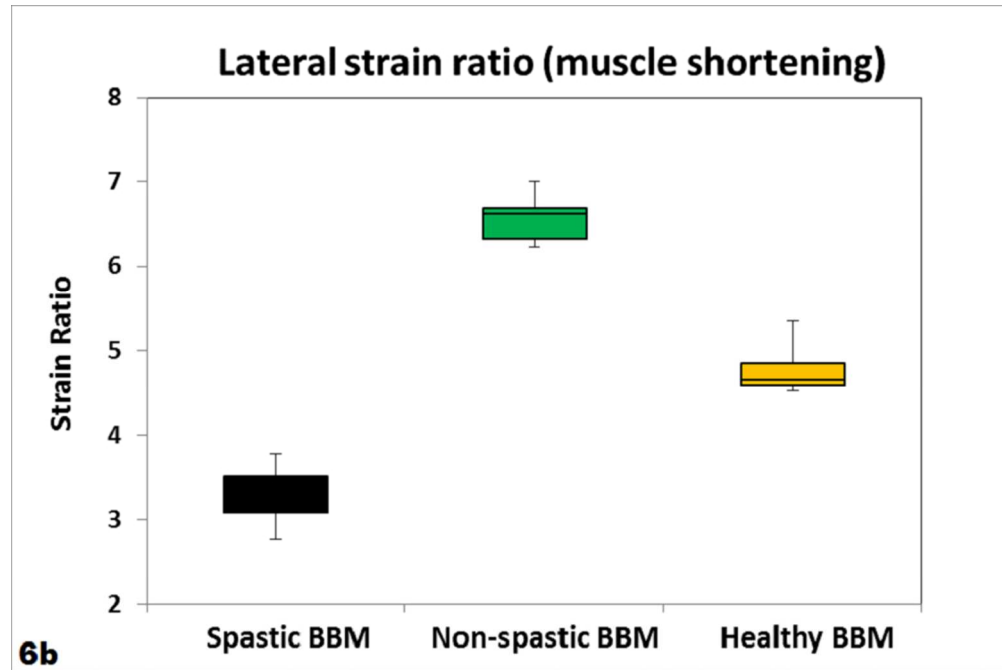


Fig. 6a-b. Box-and-whisker plots illustrate the Longitudinal strain ratios of spastic (black colored box), non-spastic (green colored box), and healthy (orange colored box) biceps brachii muscle (BBM) to reference tissue produced by elbow flexion from 0° to 90° (a) and elbow extension from 90° to 0° (b). The longitudinal strain ratio in spastic BBM is significantly lower than healthy and non-spastic BBM (Table 1). The difference in longitudinal strain ratio between healthy and non-spastic BBM at extension and flexion is also significant ($p < 0.05$).

77x51mm (300 x 300 DPI)

Author

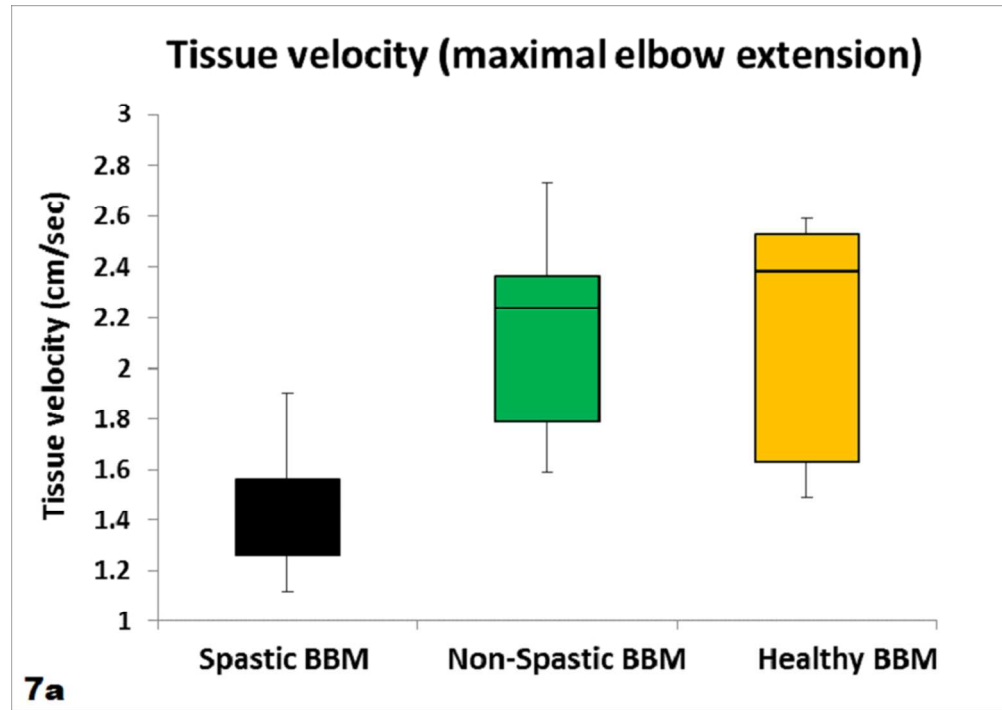


Fig. 7a-b. Box-and-whisker plots illustrate peak tissue velocity (cm/sec) in spastic (black colored box), non-spastic (green colored box), and healthy (orange colored box) biceps brachii muscle (BBM) during elbow extension from 90° to 0° (a, positive velocity value represents muscle lengthening) and during elbow flexion from 0° to 90° (b, negative velocity value represents muscle shortening). One can clearly note that the peak BBM velocity in spastic BBM is significantly lower than healthy and non-spastic BBM (Table. 1) during extension and flexion. The difference in tissue velocity between healthy and non-spastic BBM is not significant ($p > 0.05$).

77x55mm (300 x 300 DPI)

Autho

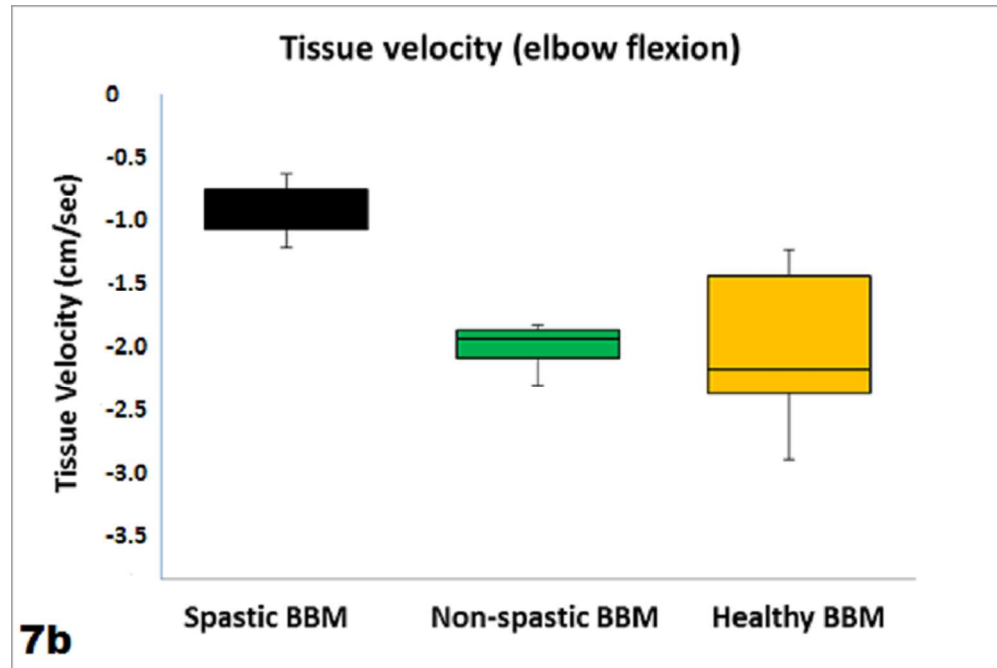


Fig. 7a-b. Box-and-whisker plots illustrate peak tissue velocity (cm/sec) in spastic (black colored box), non-spastic (green colored box), and healthy (orange colored box) biceps brachii muscle (BBM) during elbow extension from 90° to 0° (a, positive velocity value represents muscle lengthening) and during elbow flexion from 0° to 90° (b, negative velocity value represents muscle shortening). One can clearly note that the peak BBM velocity in spastic BBM is significantly lower than healthy and non-spastic BBM (Table. 1) during extension and flexion. The difference in tissue velocity between healthy and non-spastic BBM is not significant ($p>0.05$).

77x51mm (300 x 300 DPI)

Author